





# Cancer-associated POT1 mutations lead to telomere elongation without induction of a DNA damage response

Won-Tae Kim<sup>1</sup> , Kelsey Hennick<sup>1</sup> , Joshua Johnson<sup>1</sup> , Brendan Finnerty<sup>1</sup>, Seunga Choo<sup>1</sup>, Sarah B Short<sup>1</sup>, Casey Drubin<sup>1</sup>, Ryan Forster<sup>1</sup>, Mary L McMaster<sup>2</sup> & Dirk Hockemeyer<sup>1,3,4,\*</sup> 

## Abstract

Mutations in the shelterin protein POT1 are associated with chronic lymphocytic leukemia (CLL), Hodgkin lymphoma, angiosarcoma, melanoma, and other cancers. These cancer-associated POT1 (caPOT1) mutations are generally heterozygous, missense, or nonsense mutations occurring throughout the POT1 reading frame. Cancers with caPOT1 mutations have elongated telomeres and show increased genomic instability, but which of the two phenotypes promotes tumorigenesis is unclear. We tested the effects of CAS9-engineered caPOT1 mutations in human embryonic and hematopoietic stem cells (hESCs and HSCs, respectively). HSCs with caPOT1 mutations did not show overt telomere damage. *In vitro* and *in vivo* competition experiments showed the caPOT1 mutations did not confer a selective disadvantage. Since DNA damage signaling is known to affect the fitness of HSCs, the data argue that caPOT1 mutations do not cause significant telomere damage. Furthermore, hESC lines with caPOT1 mutations showed no detectable telomere damage response while showing consistent telomere elongation. Thus, caPOT1 mutations are likely selected for during cancer progression because of their ability to elongate telomeres and extend the proliferative capacity of the incipient cancer cells.

**Keywords** cancer; genome editing; human stem cells; humanized mouse models; POT1; telomeres

**Subject Categories** Cancer; DNA Replication, Recombination & Repair  
**DOI** 10.15252/embj.2020107346 | Received 18 November 2020 | Revised 9 March 2021 | Accepted 16 March 2021 | Published online 2 May 2021

**The EMBO Journal (2021) 40: e107346**

## Introduction

Recent genome-wide cancer sequencing efforts have identified mutations in the shelterin protein POT1. These cancer-associated POT1 (caPOT1) mutations are found in several cancer types,

including familial and spontaneous chronic lymphocytic leukemia (CLL) (Ramsay *et al*, 2013; Speedy *et al*, 2014), familial Hodgkin lymphoma (McMaster *et al*, 2018), and familial melanoma (Robles-Espinoza *et al*, 2014; Shi *et al*, 2014). Shelterin is the constitutive protein complex that binds the telomeric DNA sequences located at the end of linear chromosomes. The complex is comprised of six proteins, TRF1 and TRF2 that directly bind to the TTAGGG telomeric repeats, RAP1 that binds TRF2, and TIN2 that bridges TRF1 and TRF2. TIN2 is bound by the shelterin subunit TPP1 which recruits telomerase (Wang *et al*, 2007; Xin *et al*, 2007; Nandakumar *et al*, 2012; Zhong *et al*, 2012; Sexton *et al*, 2014), the reverse transcriptase that can elongate telomeres (Greider & Blackburn, 1985). Finally, POT1, the only shelterin protein that binds to the single-stranded (ss) 3' telomeric overhang (Baumann & Cech, 2001; Baumann *et al*, 2002), is recruited to telomeres by TPP1 (Ye *et al*, 2004; Xin *et al*, 2008; Rice *et al*, 2017). POT1's interaction with TPP1 is thought to be essential for the localization of POT1 to telomeres (Hockemeyer *et al*, 2007; Takai *et al*, 2011). CaPOT1 mutations are heterozygous, either missense or nonsense mutations, and occur without evidence of loss of heterozygosity or abnormal expression of the remaining wild-type alleles. They occur throughout the POT1 reading frame, including in the first two oligosaccharide–oligonucleotide binding folds (OB-folds) that mediate POT1's ability to bind the telomeric overhang, as well as in the C-terminal region of POT1's interaction domain with TPP1 (reviewed in ref. Gong *et al*, 2020).

Telomere function is linked to cancer progression through two well-established, distinct processes with disparate outcomes. First, since long-term telomere maintenance is a prerequisite for the immortal phenotype of cancer cells, telomere shortening is thought to be a tumor suppressor pathway. Second, telomere erosion occurring prior to telomerase activation can cause cancer-promoting genomic instability (Harley *et al*, 1990; Allsopp *et al*, 1992; Counter *et al*, 1992; Kim *et al*, 1994; Allsopp & Harley, 1995; Bodnar *et al*, 1998; Artandi *et al*, 2000) (reviewed in ref. Maciejowski & de Lange, 2017). Key mouse experiments have established that the cancer

1 Department of Molecular and Cell Biology, University of California, Berkeley, Berkeley, CA, USA

2 Clinical Genetics Branch, Division of Cancer Epidemiology and Genetics, National Cancer Institute, NIH, Bethesda, MD, USA

3 Chan Zuckerberg Biohub, San Francisco, CA, USA

4 Innovative Genomics Institute, University of California, Berkeley, Berkeley, CA, USA

\*Corresponding author. Tel: +1 510 664 9851; E-mail: hockemeyer@berkeley.edu

suppressing effect of telomere shortening depends on intact DNA damage checkpoint, while telomere shortening can promote genomic instability and cancer progression in checkpoint-deficient cells (Greenberg *et al*, 1999; Artandi & DePinho, 2000; Artandi *et al*, 2000).

POT1 contributes to both telomere maintenance and telomere protection. First, POT1 regulates telomere length by binding the telomeric overhang and modulating telomerase-mediated telomere extension. Depletion of POT1 with shRNAs or overexpression of POT1 $\Delta$ OB, a form of POT1 lacking its first OB-fold and unable to bind ss-DNA, leads to telomere elongation in telomerase-positive cells (Loayza & de Lange, 2003; Hockemeyer *et al*, 2005; Lei *et al*, 2005; Wang *et al*, 2007). Second, POT1 protects the telomere against a DNA damage response by binding to the single-stranded telomeric 3' overhang (Hockemeyer *et al*, 2005; Hockemeyer *et al*, 2006). This binding prevents the overhang from being detected by RPA, which would lead to initiation of the ATR-mediated DNA damage response (Denchi & de Lange, 2007). Loss of POT1 also elicits a change in the length of the telomeric overhang, telomere-driven genomic instability, and an ATR-mediated cell cycle arrest (Denchi & de Lange, 2007). It is unclear whether the positive selection for caPOT1 mutations during cancer progression is due to loss of telomere length control or loss of telomere protection. Both increased telomere length and increased genomic instability have been reported in cancer samples with caPOT1 mutations (Ramsay *et al*, 2013; Robles-Espinoza *et al*, 2014; Shi *et al*, 2014; McMaster *et al*, 2018), making it difficult to assess which of these phenotypes drove the early expansion of cells with caPOT1 mutations and which is a “bystander phenotype”.

Previous approaches have analyzed the phenotypes associated with caPOT1 mutations in mice (Pinzaru *et al*, 2016). Mice have very long telomeres, and telomerase generally does not restrict the proliferative capacity of mouse cells (Kipling & Cooke, 1990; Blasco *et al*, 1997). Therefore, the impact of caPOT1 mutations on the processes driving an incipient cancer to become immortal cannot be addressed in mice. Nevertheless, analysis of mice engineered to carry homozygous POT1 mutations found in cutaneous T-cell lymphoma (CTCL) showed that these mutations can induce an ATR-mediated DNA damage response. When assayed in a p53-negative cancer setting, this telomere DNA damage response will eventually lead to the long-term attenuation of ATR signaling, which has been proposed to promote cancer development (Pinzaru *et al*, 2016).

In addition, caPOT1 mutations have been studied in human cells either by overexpression of caPOT1 alleles combined with and without the simultaneous depletion of wild-type POT1 in cancer cells or by engineering the homozygous mutations in cancer cell lines (Pinzaru *et al*, 2016; Chen *et al*, 2017; Gu *et al*, 2017; McMaster *et al*, 2018; Pinzaru *et al*, 2020). Under these conditions, POT1 mutations lead to telomere elongation and telomere deprotection. Thus, these experiments also did not address the question of which of these phenotypes is critical for cancer progression.

Here, we dissect how caPOT1 mutations can promote cancer progression in human cells. To do this, we engineered caPOT1 mutations into human primary stem cells in the disease-relevant heterozygous setting. Our *in vitro* and long-term xenograft experiments demonstrate that cells bearing heterozygous mutations do not have an increased DNA damage response at telomeres. Also, the mutant cells are not selected against but persist over time. This lack

of a selective pressure against POT1 mutant cells in a checkpoint-proficient setting argues against a DNA damage response driving cancer progression. In contrast, caPOT1 mutations resulted in telomere elongation. Specifically, we assessed the impact of heterozygosity for two caPOT1 mutations, Y223C and Q623H, on telomere length and telomere protection in human pluripotent stem cells. In this system, we also find that the caPOT1 mutations do not trigger a telomere DNA damage response, yet result in telomere elongation over time.

## Results

### The Q623H caPOT1 mutation does not cause telomere deprotection in human pluripotent stem cells

Previous studies to address the mechanism by which caPOT1 mutations promote cancer relied on either overexpression experiments or analysis of cells with homozygous POT1 mutations. In order to generate a more accurate model, we engineered human embryonic stem cells (hESCs) to carry caPOT1 mutations in the disease-relevant heterozygous setting. We initially focused on two caPOT1 mutations, Y223C and Q623H, which have been reported to lead to a DNA damage response when overexpressed in cancer cells (Pinzaru *et al*, 2016; Chen *et al*, 2017; Gu *et al*, 2017; McMaster *et al*, 2018). Using homology-directed repair, we successfully generated heterozygous (POT1<sup>WT/Q623H</sup>) and homozygous (POT1<sup>Q623H/Q623H</sup>) knock-in hESCs (Fig 1A and Appendix Fig S1). However, this conventional genome editing approach was not successful in generating POT1<sup>WT/Y223C</sup> hESCs. Two independent targeting experiments resulted in two cell lines with the Y223C allele, but both hESC lines carried a frameshift mutation on the second allele, resulting in POT1 compound heterozygous cell lines (POT1<sup>Y223C/-</sup>) (Appendix Fig S1). All cells grew normally, retained a pluripotent state, and were passaged and maintained in parallel without any obvious defects. Next, we analyzed these cells for the presence of telomere-dysfunction induced foci (TIFs) (d'Adda di Fagagna *et al*, 2003; Takai *et al*, 2003) to determine whether caPOT1 mutations elicit a DNA damage response. Here, we found that the Q623H mutation did not induce a DNA damage response at telomeres in either heterozygous or homozygous cells. Interestingly, we found that the compound heterozygous cells with the Y223C mutation showed a robust TIF response (Fig 1B and C). This result agrees with previously reported loss-of-function phenotypes for POT1. Therefore, while not informative for the phenotype of the heterozygous caPOT1 mutations, this result served as a positive control for these experiments. Similarly, we found that the Q623H mutation did not lead to chromosomal changes, such as chromosome fusions or fragile telomeres. POT1<sup>Y223C/-</sup> hESCs showed a mild increase in fragile telomeres (Fig 1D and E). These data demonstrate that the Q623H caPOT1 mutation does not elicit a DNA damage response or aberrant telomere repair in hESCs.

### The Q623H POT1 mutation leads to telomere elongation in pluripotent stem cells

The lack of a significant increase in TIF responses in Q623H cells prompted us to analyze changes in telomere length as the potential

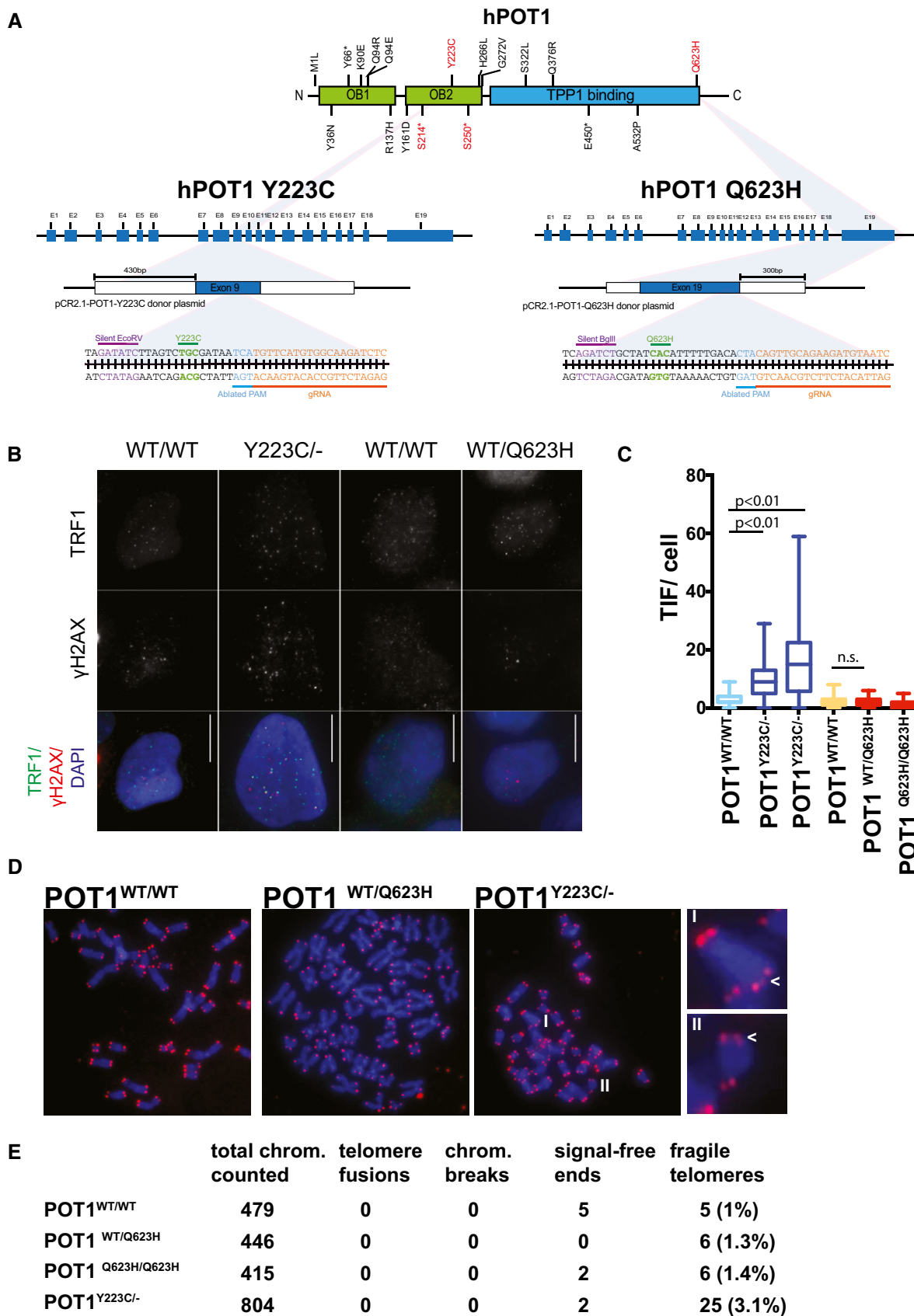


Figure 1.

**Figure 1. The Q623H caPOT1 mutation does not induce a DNA damage response at telomeres.**

- A Schematic of the POT1 locus and editing strategy used to engineer hESCs with the Y223C and Q623H caPOT1 mutations.
- B Representative images for the TIF analysis shown in (C). Shown are POT1<sup>Y223C/-</sup> hESCs and an unedited wild-type hESC clone (WT/WT) isolated in parallel, as well as a POT1<sup>WT/Q623H</sup> hESC and a contemporaneously isolated hESC clones (WT/WT). Scale bars = 10 μm.
- C Box and whisker plot (showing min, max, and average) quantifying telomere-dysfunction induced foci (TIF) in two POT1<sup>Y223C/-</sup> hESC lines, one POT1<sup>Q623H/Q623H</sup>, and one POT1<sup>WT/Q623H</sup> hESC lines compared to wild-type unedited control hESCs. Cells were analyzed 3 months post-targeting. Cells were stained for TRF1 and γ-H2Ax. POT1<sup>Y223C/-</sup> cells have increased TIFs compared to an unedited wild-type cell clone, isolated and cultured in parallel ( $P < 0.01$ , two-tailed Mann–Whitney test, one biological replicate).
- D Images of telomere and centromere FISH on metaphase spreads of cell lines as in (B). Cy3 Tel-C PNA probes were used. Arrows indicate chromosomal abnormalities.
- E Quantification of chromosomal abnormalities as determined by FISH analysis in (D).

cancer-promoting phenotype of caPOT1 mutations. POT1<sup>Y223C/-</sup> cells had significantly elongated telomeres compared to wild-type control cells (Appendix Fig S2). This telomere elongation occurred rapidly, as it was already detectable at the earliest time point that we could analyze. In comparison, POT1<sup>Q623H/Q623H</sup> and POT1<sup>WT/Q623H</sup> initially had telomeres of the same length as those of the unedited control cells. However, while unedited control cells were stable over time, both POT1<sup>Q623H/Q623H</sup> and POT1<sup>WT/Q623H</sup> cells showed slow but progressive telomere elongation (Fig 2A and B, and Appendix Fig S2). From this result, we conclude that the Q623H caPOT1 mutations can drive telomere elongation without an observable increase in DNA damage response.

**The Y223C caPOT1 mutation does not cause telomere deprotection but telomere elongation**

The Q623H caPOT1 mutation did not cause a DNA damage response at telomeres in hESCs when present in the heterozygous genomic configuration found in patients. Yet, we demonstrate that the Q623H caPOT1 mutations lead to telomere elongation in hESCs.

Next, we wanted to test whether telomere elongation is a common phenotype of caPOT1 mutations. As outlined above, we initially intended to generate hESCs with the Y223C heterozygous caPOT1 mutation. Unfortunately, several attempts resulted only in compound heterozygous cells instead of the disease-relevant heterozygous POT1 mutations. To overcome this challenge and to finally generate POT1<sup>WT/Y223C</sup> cells, we devised a novel two-step editing strategy to generate these mutations (Fig 3A). In a first step, we used CAS9-mediated homologous repair to integrate a puromycin resistance cassette into the POT1 locus and simultaneously generate the proximal Y223C mutation. After genotyping and expanding the edited cells, we scarlessly excised the puromycin cassette using the simultaneous expression of two sgRNAs precisely targeting sites flanking the cassette, so that successful excision leaves behind only the intended Y223C mutation (Fig 3 and Appendix Fig S3A–D). Having generated these cells, we again confirmed that caPOT1 mutations do not induce a TIF response (Fig 3B and C). Yet, cells carrying a Y223C mutation are capable of responding to loss of POT1 at telomeres with the induction of TIFs, as lentiviral transduction with TPP1ΔPBD, an allele of TPP1 missing

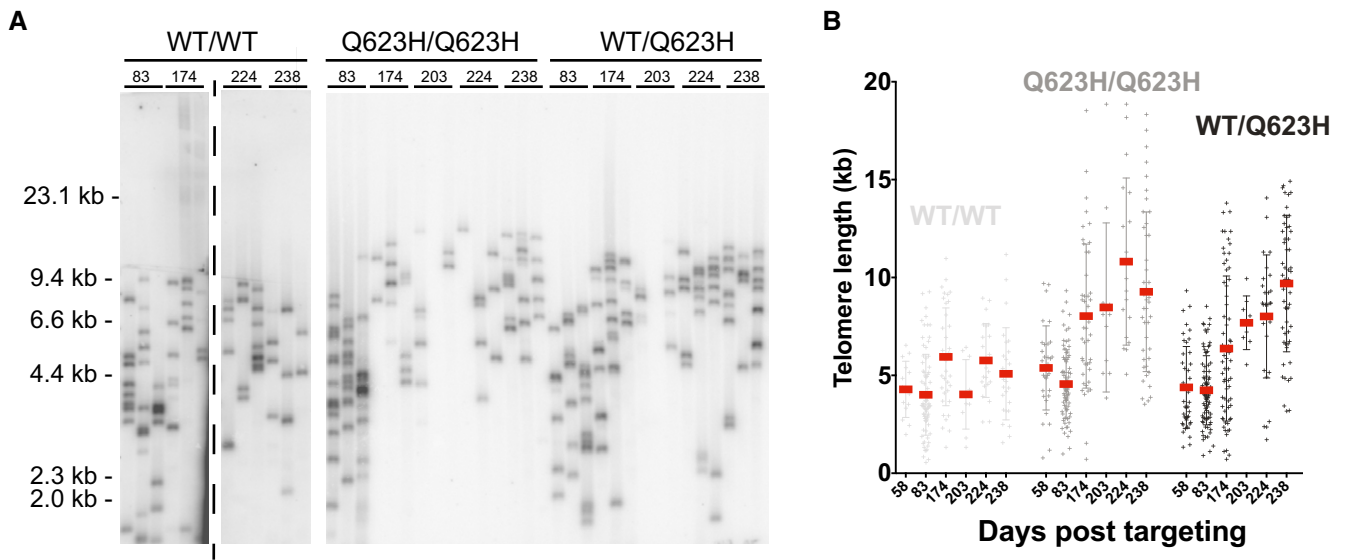


**Figure 2. The Q623H caPOT1 mutation leads to elongation in hESCs.**

- A Single telomere length analysis (STELA) for POT1<sup>Q623H/Q623H</sup> and POT1<sup>WT/Q623H</sup> hESCs compared an unedited wild-type hESC clone that was isolated and cultured in parallel to the edited clones. Numbers above the radiograph indicated days after editing the respective POT1 mutations.
- B Quantification of telomere length data from two STELA experiments using the same genomic DNA, shown in (A) and (Appendix Fig S2C). Indicated in red is the mean telomere length, and the error bars indicate the standard deviation.

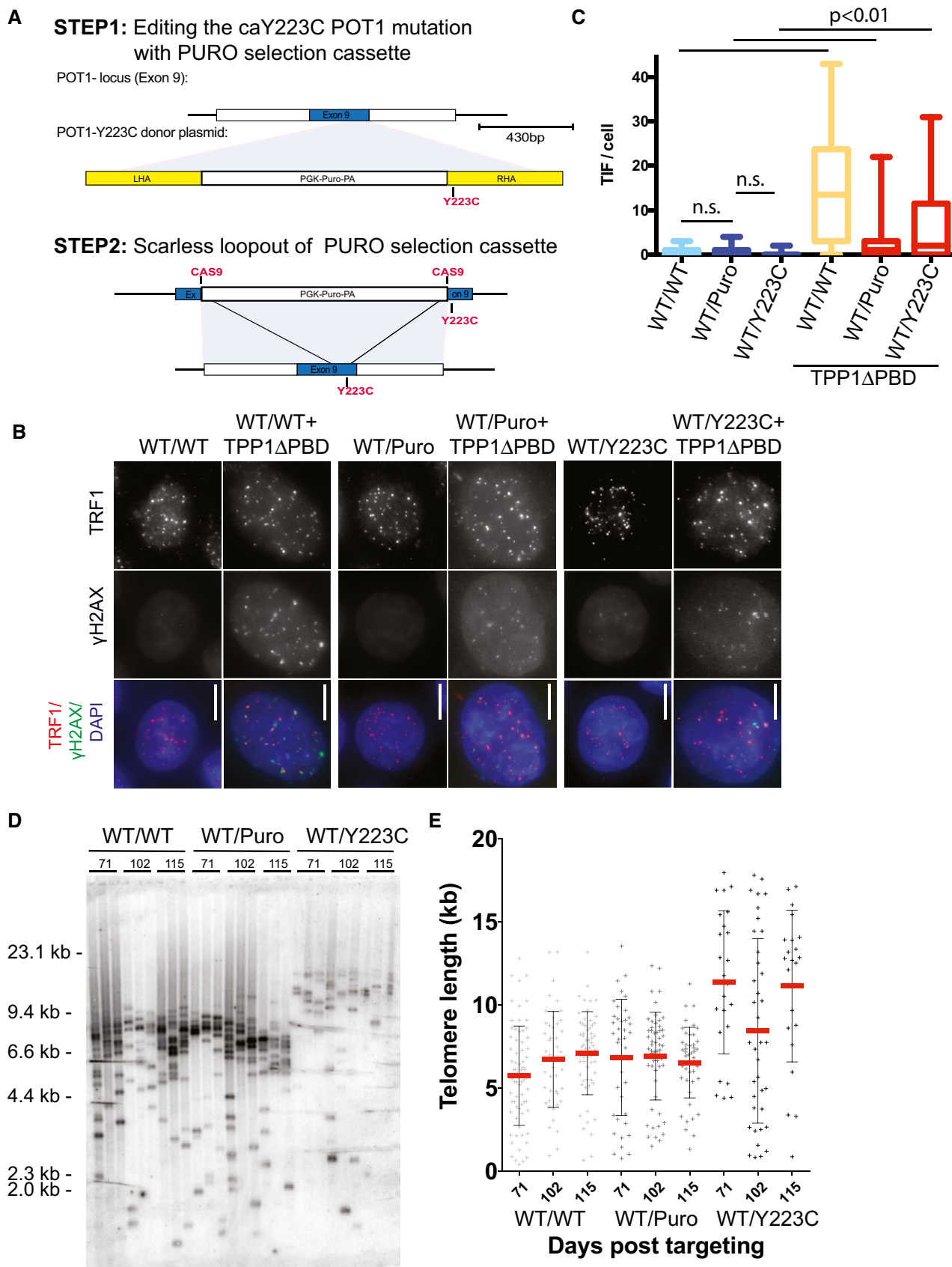


Figure 3.

**Figure 3. A heterozygous Y223C caPOT1 mutation does not induce a DNA damage response at telomeres, but elongates telomeres.**

- A Schematic for the "scarless loopout" strategy used to generate POT1<sup>WT/Y223C</sup> in hESCs.
- B TIF analysis of wild-type, POT1<sup>WT/Y223C</sup> hESCs, and the indicated controls using antibodies against TRF1 and  $\gamma$ -H2AX. Scale bars = 10  $\mu$ m. Lentiviral expression of TPP1 $\Delta$ PBD served as a positive control to demonstrate that cells have an intact telomere DNA damage response. TPP1 $\Delta$ PBD-infected cells were analyzed 72 h post-infection and without selection.
- C Box and whisker plot (showing min, max, and average) quantifying the fraction of TIF-positive telomeres per cells as shown in (B) (two-tailed Mann–Whitney test, one biological replicate).
- D STELA showing telomeres of POT1<sup>WT/Y223C</sup>, POT1<sup>WT/Puro</sup>, and an untargeted control hESC clone that was isolated and cultured in parallel to the edited clone.
- E Quantification of two STELA experiments, including that shown in (D). Indicated in red is the mean telomere length, and the error bars indicate the standard deviation.

the POT1 binding domain, triggered a strong TIF response as expected. Similar to the Q623H mutation, the Y223C mutation did not induce gross chromosomal abnormalities or fragile telomeres (Appendix Fig S3E). Importantly, telomere length analysis of cells with the Y223C mutations showed elongated telomeres compared to wild-type cells (Fig 3D and E). From this, we conclude that caPOT1 mutations can lead to telomere elongation in cells that do not show an increased telomere DNA damage response at telomeres.

**Hematopoietic stem cells with POT1 mutations proliferate and differentiate normally**

It is possible that the damage response in caPOT1 cells is below our detection limit and/or that the sensitivity to DNA damage is cell type-specific with hESCs potentially having a higher DNA damage tolerance. Therefore, we also evaluated the effect of caPOT1 mutations in human primary hematopoietic cells, the cell type that gives rise to CLL. We accomplished this by genetically engineering caPOT1 mutations into hCD34<sup>+</sup> human hematopoietic stem cells (hCD34<sup>+</sup> cells). There are several caPOT1 mutations reported in exon 9, including two premature stop mutations at positions 214 and 250 in CLL and other cancers (Ramsay *et al*, 2013). To model these premature stop mutations, we screened for single guide (sg)RNAs that efficiently cut in exon 9 to yield CAS9-mediated gene disruption. First, we screened a panel of sgRNAs in K562 and then in CD34<sup>+</sup> cells to identify sgRNAs that efficiently cut in exon 9 of POT1 (Appendix Fig S4A–C). We identified two sgRNAs that resulted in approximately 20–25% gene disruption by insertions and deletions (in/dels) at the sgRNA cut site, generating premature stop mutation alleles resembling reported cancer-associated nonsense mutations in between amino acids 214 and 250. Nucleofection of the same sgRNAs into hCD34<sup>+</sup> cells resulted in 17% in/del generation with a similar allele spectrum when assayed 48 h after nucleofection (Fig 4A and B and Appendix Fig S4D–F).

We used this primary cell system to test the hypothesis that caPOT1 mutations result in a DNA damage response that causes a selective pressure forcing the attenuation of the ATR response as has been proposed for CTCL (Pinzaru *et al*, 2016). We screened for such a selective disadvantage by comparing the proliferative capacity of edited cells to wild-type controls. We cultured a pool of POT1-edited hCD34<sup>+</sup> cells containing 17% of POT1-edited cells for two weeks using well-established differentiation conditions for HSCs (Giarratana *et al*, 2005; DeWitt *et al*, 2016; Fig 4C). Cells edited at the previously established neutral AAVS1 locus served as technical controls for all experiments (Lombardo *et al*, 2007; Hockemeyer *et al*, 2009; DeKolver *et al*, 2010; De Ravin *et al*, 2016). Genotyping

of single cell-derived clones revealed that cells with heterozygous POT1 mutations were not selected against, as they could be detected with a similar overall frequency of 18.5% (Fig 4D and E) to that of the initial pool of edited hCD34<sup>+</sup> cells. We failed to detect cell clones with homozygous POT1 mutations. Again, the lack of any overt proliferation defect of POT1 mutant cells in this experiment argues that heterozygous POT1 mutations do not elicit a DNA damage response even when engineered in DNA repair-proficient human primary hematopoietic cells.

**Xenografted hematopoietic stem cells with POT1 mutations are not selected against *in vivo***

Although the wild-type and the mutation-bearing colonies did not reveal any overt differences in the previous short-term *in vitro* differentiation paradigm, we reasoned that a DNA damage response might be so minor that it would only become apparent if cells were differentiated for longer periods of time or into more mature cell types. To test this, we performed long-term xenograft experiments of POT1-edited cells and assayed their proliferative capacity. We measured the allele frequency of POT1 mutations in comparison with the wild-type allele over time in the bone marrow of long-term engrafted mice (Fig 5A). This approach has previously been established to be a very sensitive assay to reveal changes of cellular fitness of human hematopoietic cells *in vivo* (McIntosh *et al*, 2015). Again, cells edited at the neutral safe harbor AAVS1 locus served as technical controls for all experiments. POT1 and AAVS1-edited hCD34<sup>+</sup> cells were injected into NBSGW immune-deficient mice via tail vein injection. Four months after transplantation, hCD34<sup>+</sup> HSCs originating from long-term engrafted human cells were isolated and sorted from the recipient bone marrow and then differentiated into colony-forming units. In addition, we separated the engrafted hCD45<sup>+</sup> fraction into either CD19<sup>+</sup> or CD19<sup>-</sup> populations (Fig 5 and Appendix Fig S4G and H). CD19 is a pan-B-cell marker, and B cells are the cell of origin for CLL. Next-generation sequencing (NGS) of these cells revealed POT1 edits in all cell types analyzed (Fig 5B and C and Appendix Fig S5A and B). Moreover, the allele frequency of POT1 mutations in all cell types was similar to that of the initial pool of cells before transplantation. We confirmed these findings for the second sgRNA cutting in exon 9 and closer to the Q214X caPOT1 nonsense mutation using POT1 sgRNA-2 (Appendix Fig S5C and D). This result again argues that POT1 mutations do not lead to a DNA damage response that would elicit a strong selective pressure against cells. In addition to this bulk population analysis, we also *in vitro* differentiated the CD34<sup>+</sup> cells isolated from recipient mice and assessed their genotype at the POT1 mutation locus



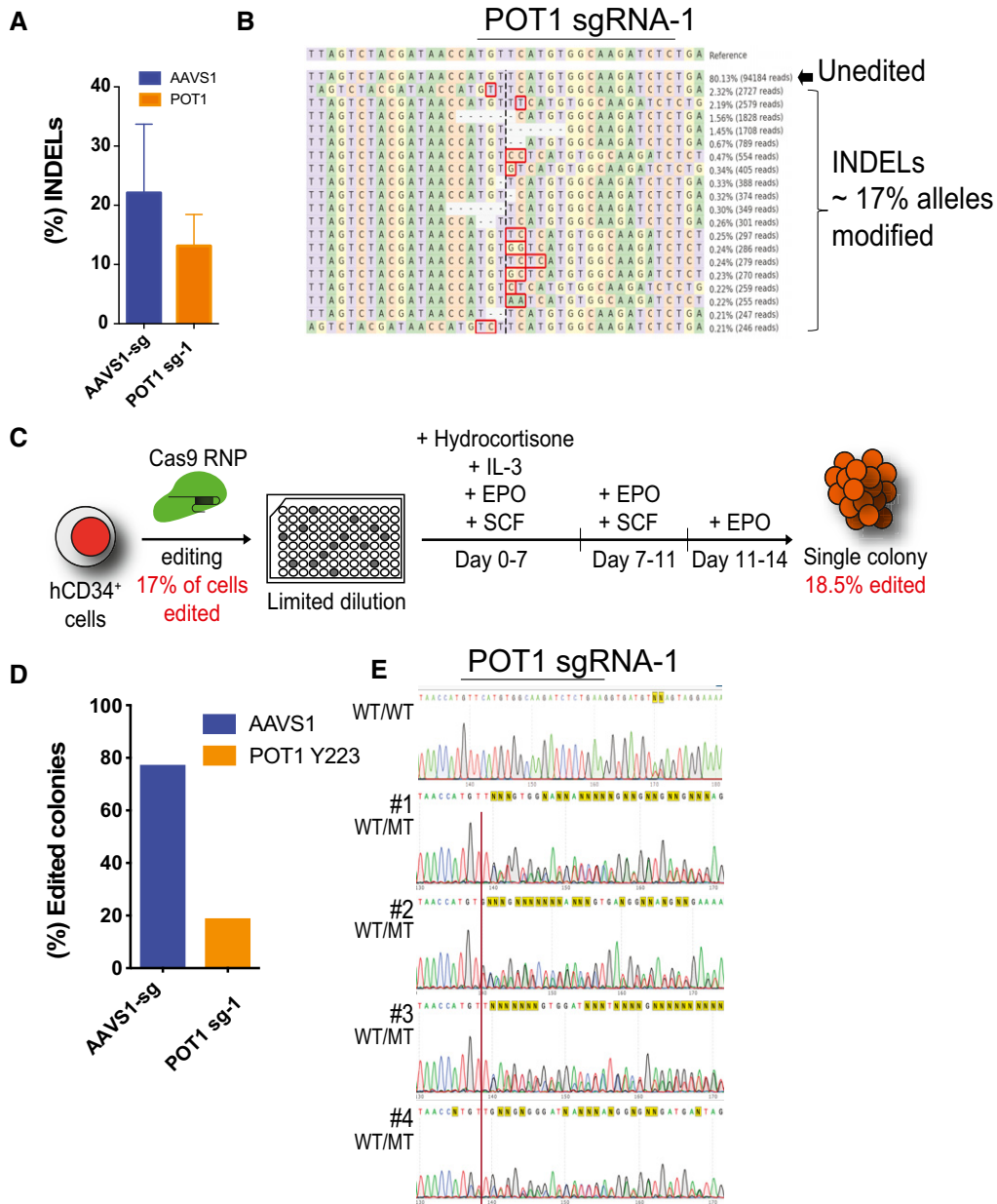
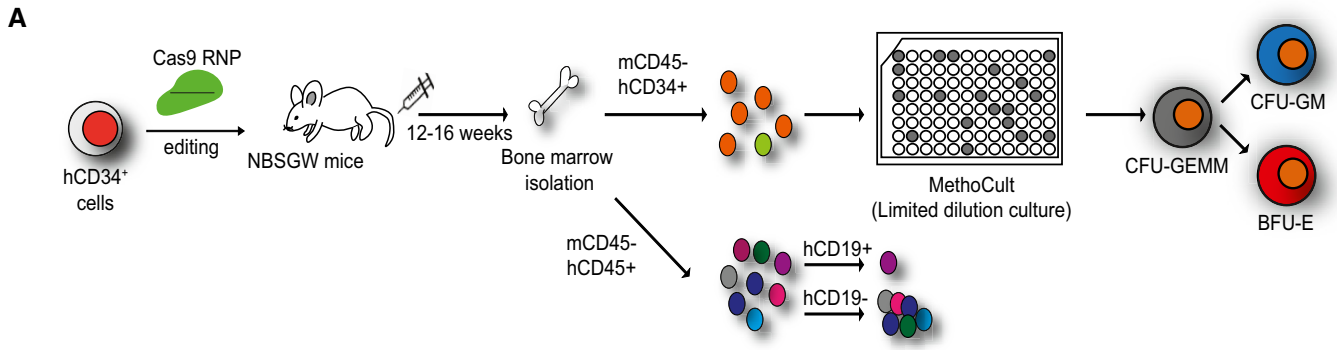


**Figure 4. POT1 mutations are tolerated in hematopoietic stem and differentiated cells *in vitro*.**

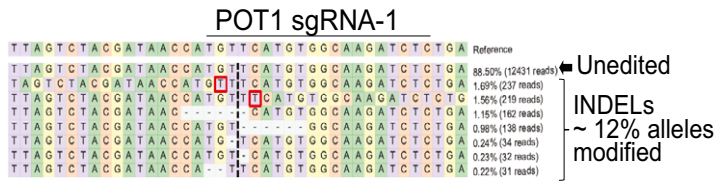
- A Editing efficiency of hCD34<sup>+</sup> cells at the AAVS1 control locus or in exon 9 of POT1 using sgRNA-1. Shown are the average results of the three different nucleofection experiments of CD34<sup>+</sup> cells. Error bars represent the standard deviation.
- B Plot showing frequencies of different alleles determined by NGS two days after nucleofection. The vertical dashed line shows the site of CAS9 cut, and the base pairs noted in red show insertion. A dash inside a gray box indicates a deleted base pair.
- C Schematic of the differentiation protocol for edited CD34<sup>+</sup> cells into erythroid cells. After editing, hCD34<sup>+</sup> cells were cultured for 7 days in IMDM containing indicated chemicals and cytokines. Next, culture medium was replaced with IMDM containing same cytokines except for hydrocortisone and IL-3 for another 4 days. The differentiated cells were cultured for 3 days more days with in IMDM supplemented with 5% human AB serum, heparin, insulin, transferrin, and EPO before genomic DNA was extracted for genotyping.
- D Quantification of edited or unedited colonies isolated in the *in vitro* differentiation described in (C). WT: wild-type and MT: mutant.
- E Representative Sanger sequencing chromatogram of four hCD34<sup>+</sup> cell-derived heterozygous POT1-edited colonies shown in (C) and (D). WT: wild-type and MT: mutant. The red line indicates the CAS9 cleavage site, 3 nt upstream of the PAM site.

(Appendix Fig S5E). This *in vitro* differentiation paradigm results in colonies the three characteristic morphologies for colony-forming units (CFU) of different hemopoietic lineages, CFU-GEMM (common

myeloid progenitor cells: granulocyte, erythrocyte, monocyte, megakaryocyte), BFU-E colonies (burst forming unit-erythroid), and granulocyte–macrophage progenitor colonies (CFU-GM), that can be



**B** CD34+ cells before engraftment



**C** isolated from mouse BM after week 16

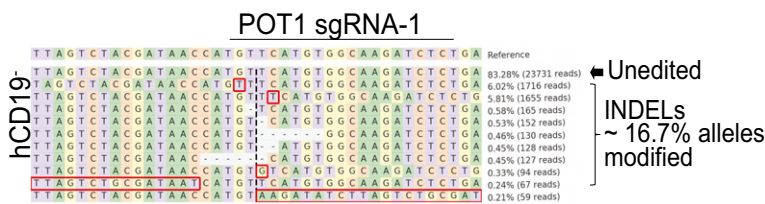
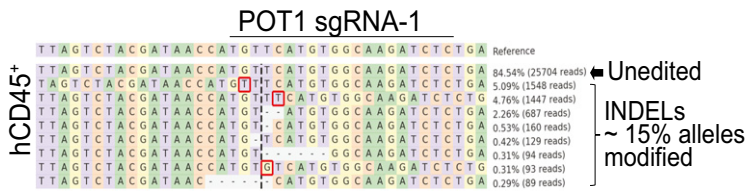
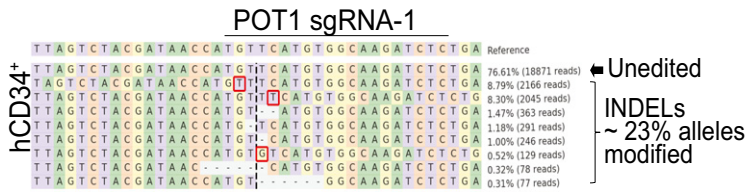
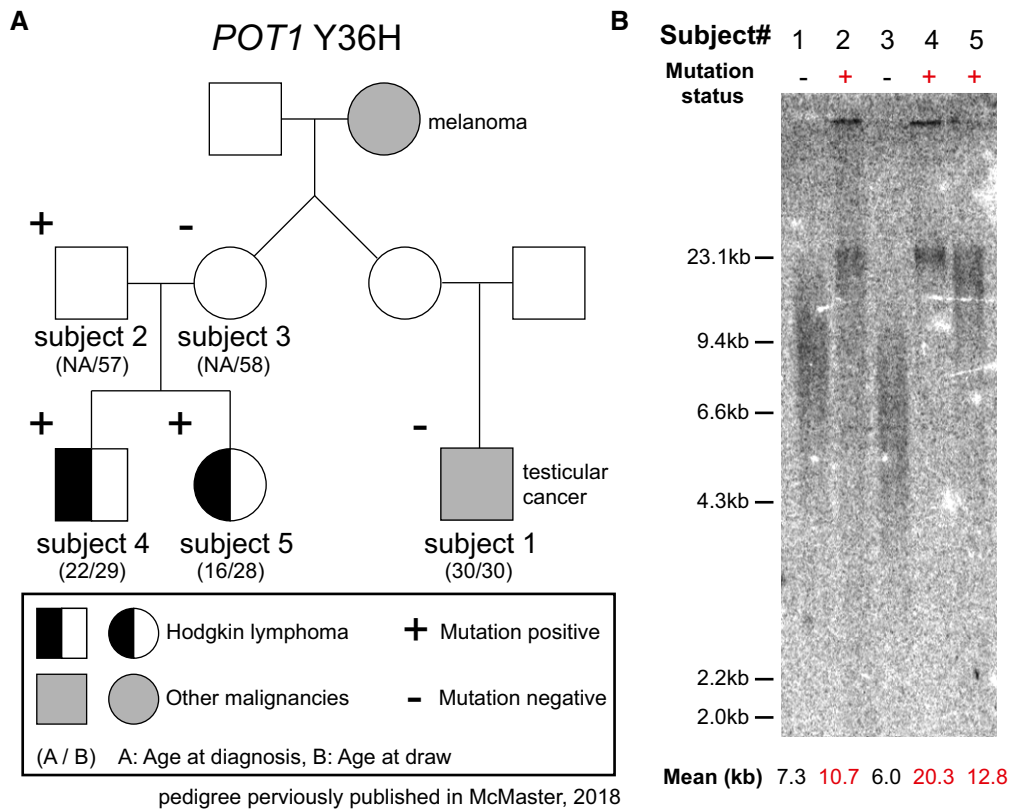


Figure 5.



**Figure 5. POT1 mutations are not selected against *in vivo*.**

A Experimental outline for the xenografting of CAS9-edited hCD34<sup>+</sup> cells into mice, isolation of human cells from the bone marrow, and sequential *in vitro* differentiation.  
 B Editing outcomes of hCD34<sup>+</sup> cells nucleofected with POT1 sgRNA-1 before transplantation determined by NGS.  
 C Representative genotyping outcomes of hCD34<sup>+</sup> cells nucleofected sgRNA-1, xenografted, and isolated from the bone marrow 16 weeks after transplantation into mice determined by NGS.  
 Data information: (B, C) The vertical dashed line shows the site of CAS9 cut, and the base pairs noted in red show insertion. A dash inside a gray box indicates a deleted base pair.



**Figure 6. The familial caPOT1 Y36H mutation leads to telomere elongation in somatic tissues.**

A A pedigree of a Hodgkin lymphoma family with POT1 Y36H mutation (adapted from and previously published in McMaster *et al*, 2018). More details of the subjects are listed in Appendix Table S1.  
 B Telomere restriction fragment assay for the five subjects shown in (A). Mean telomere length is indicated.

easily distinguished based on their morphology (Appendix Fig S5F). Importantly, this colony assay also readily revealed heterozygous POT1 edits (Appendix Fig S5G–I).

**CaPOT1 mutations lead to telomere elongation in familial non-Hodgkin’s lymphoma**

Familial caPOT1 mutations have been reported to lead to telomere elongation in somatic non-cancerous tissue of cancer patients compared to the somatic tissue of age matched controls (Shi *et al*, 2014). To further corroborate these findings and to directly follow how telomere length changes in families with caPOT1 mutations, we measured telomere length differences between family members of a recently reported family that carries a

caPOT1 Y36H mutation (McMaster *et al*, 2018) (Fig 6A). We analyzed peripheral lymphocyte DNA from 3 carriers and 2 relatives without the mutation. Telomere length measurements in this family revealed that telomeres in POT1 Y36H carriers were elongated compared to somatic telomeres in family members without the mutation (Fig 6B). Interestingly, telomeres in the third generation of carriers in this family (McMaster *et al*, 2018) showed longer telomeres than the parental carrier. This could suggest that the elongated telomeres are passed through the germline. Together, the pronounced telomere elongation in somatic tissues in combination with the apparent lack of phenotypes expected from a chronic DNA damage response argues that in somatic tissues, telomere elongation is uncoupled from a DNA damage response in the cancer tissue.

## Discussion

### CaPOT1 mutations in the DNA-binding domain and in the TPP1 interaction domain cause telomere elongation but not a telomere DNA damage response

A fascinating feature of caPOT1 mutations is their distribution as nonsense or missense mutations throughout the entire reading frame of POT1. For example, caPOT1 mutations include a premature stop at position 250 in the second OB-fold of POT1; Y223C, an amino acid substitution predicted to impair POT1's ss-binding ability; and Q623H, a mutation at the C-terminus where POT1 interacts with TPP1. Our experiments demonstrate that heterozygous cells carrying either Q623H or Y223C mutation have elongated telomeres, without evidence of a DNA damage response. However, our experiments also detect important differences between these mutants. Telomere elongation appears to be faster in cells with the heterozygous Y223C mutation than in cells with heterozygous Q623H mutation. Similarly, compound heterozygous POT1<sup>Y223C/-</sup> cells show fast telomere elongation and a strong TIF response, while cells homozygous for the Q623H mutation do not have TIFs and only a moderate rate of telomere elongation. This complexity is surprising and warrants the analysis of additional caPOT1 mutations. Our finding that POT1<sup>Y223C/-</sup> cells have TIFs agrees with the DNA damage response seen in mice engineered with homozygous POT1a mutations (Hockemeyer *et al*, 2006; Denchi & de Lange, 2007; Pinzaru *et al*, 2016). Both caPOT1 mutations lead to telomere elongation when engineered in a disease-relevant heterozygous setting. Thus, we propose that telomere elongation is the common phenotype of caPOT1 mutations.

### How do caPOT1 mutations drive cancer progression in specific cancer types?

Our data suggest that caPOT1 mutations can drive cancer progression by elongating telomeres in the incipient cancer cells. This conclusion is consistent with the tumor spectrum in which caPOT1 mutations most frequently occur: familial and sporadic CLL as well as familial melanoma. Despite very different malignancies, telomere length has been established to be a key driver of disease progression in both cancer types (Horn *et al*, 2013; Huang *et al*, 2013; Shain *et al*, 2015; Chiba *et al*, 2017). Individuals with constitutively long telomeres are at a greater risk of developing melanoma (Rode *et al*, 2016). The simplest interpretation of how familial caPOT1 mutations drive cancer is that these mutations elongate the overall telomere length. The elongated telomeres in these patients grant the incipient cancer cells an extended proliferative capacity, expanding the population of cells that can acquire additional mutations required for cancer progression. This model is supported by the increased telomere length in the families with POT1 mutations (reviewed in ref. Gong *et al*, 2020). Thus, we propose that POT1 mutations can be found in familial CLL and melanoma because here caPOT1 mutations are passed through telomerase-positive cells of the early embryo (Wright *et al*, 1996), where they exert their cancer-promoting telomere elongation.

This concept that familial mutations in shelterin components can drive cancer by elongating telomeres is independently confirmed by the identification of cancer-causing mutations in TIN2, encoding the shelterin protein TIN2. As described here for the Y36H caPOT1

mutation, familial TIN2 mutations also cause cancer and long germline telomeres without affecting telomere protection (He *et al*, 2020; Schmutz *et al*, 2020). Together, these results highlight the tumor suppressive role of shelterin in curtailing aberrant telomere elongation.

The mechanism by which sporadic caPOT1 mutations drive cancer seems to be more complex. An intriguing observation is that sporadic caPOT1 mutations have been reported in CLL but not in melanoma cases. It is possible that the high overall mutation burden in melanoma makes it difficult to assign functional relevance to POT1 mutations. Alternatively, the difference in POT1 mutation frequency in sporadic CLL and melanoma could be caused by a difference in the telomerase levels of the tumor-initiating cell types. In CLL, the affected cells express telomerase activity, although at a low level (Kolquist *et al*, 1998), and thus, caPOT1 mutations can lead to telomere elongation. In contrast, in telomerase-negative melanocytes (Rudolph *et al*, 2000), a sporadic caPOT1 mutation will lead to neither telomere elongation nor selective advantage.

As Lin and colleagues point out (Lin *et al*, 2014), POT1 mutations are almost exclusively associated with unmutated IGHV genes in CLL, but these cases do not show increased genomic instability or critically short telomeres (Lin *et al*, 2014). Also, caPOT1 mutations are not specifically enriched for the loss of p53 which, again, points to an unusual etiology of CLL with POT1 mutations. In CLL, telomere shortening has been shown to be an early feature of disease progression, an observation that at first glance is counterintuitive to our proposed mechanism of caPOT1 mutation promoting telomere elongation (Damble *et al*, 2004; Roos *et al*, 2008; Rossi *et al*, 2009; Lin *et al*, 2010; Escudero *et al*, 2019). However, it is possible that caPOT1 mutations can take effect in a later stage of CLL when telomeres are already short. This is because cancer cell survival is balanced between genomic instability leading to further mutagenesis and the proliferative advantage granted by telomere elongation, as well as short yet stable telomeres. Here, we propose that caPOT1 mutations can have a strong impact on the immediate survival of CLL cells once telomeres have substantially shortened even if there is only a small change in telomere length.

Ultimately, resolving the complexities of how changes in telomere length impact cancer progression will require us to follow human cells with caPOT1 mutations in the proper genetic context and ideally *in vivo*. In the case of CLL, this would require a system that includes the CLL-relevant driver mutations and that recapitulates the telomere length and proliferation dynamics of CLL. It seems possible that the effect of a caPOT1 mutation is more prominent in cells with critically short telomeres, since a slight increase in telomerase activity is expected to increase the proliferative capacity of cells with caPOT1 mutations. The humanized mouse model for caPOT1 mutations presented in this paper could be the starting point for an experimental system to tackle these questions *in vivo*. Independent of such future studies, it seems clear that mutations in TERT (Horn *et al*, 2013; Huang *et al*, 2013), TIN2 (He *et al*, 2020; Schmutz *et al*, 2020), and POT1 (Ramsay *et al*, 2013; Robles-Espinosa *et al*, 2014; Shi *et al*, 2014; Speedy *et al*, 2014; McMaster *et al*, 2018) can cause telomere elongation and cancer. This cancer-promoting phenotype of long telomeres greatly complicates proposals to use telomere elongation as a "therapeutic intervention" designed to attenuate aging or age-associated diseases (Chakravarti *et al*, 2021).

## Materials and Methods

### Cell culture and cryopreservation

Human bone marrow CD34<sup>+</sup> hematopoietic stem/progenitor cells were obtained from AllCells and Fred Hutchinson Cancer Research Center. CD34<sup>+</sup> cells were maintained in StemSpan SFEM II medium supplemented with CC110 (StemCell Technologies). K562 cells were cultured in IMDM supplemented with 10% FBS and 1% penicillin/streptomycin. Frozen stocks were prepared with 10% DMSO and 30% FBS in K562 medium and stored in liquid nitrogen prior to use. Genome editing experiments in hESCs were performed as previously described (Hockemeyer *et al*, 2009; Soldner *et al*, 2009; Hockemeyer *et al*, 2011) in the WIBR#3 line (Lengner *et al*, 2010) and NIH stem cell registry # 0079. Cell culture was carried out as previously described in Boyle *et al* (2020).

### Guide RNA design and preparation

For hCD34<sup>+</sup> experiments, POT1 OB-fold and AAVS1 loci were targeted by sgRNA designed using the following open web tool: <https://zlab.bio/guide-design-resources>. Oligos containing the T7 promoter, a specific sgRNA sequence (AAVS1 oligo, POT1 sgRNA-1 oligo, POT1 sgRNA-2 oligo), and a non-variable region of the sgRNA were assembled with a primer containing the reverse complement sequence of the non-variable region of the sgRNA (T7RevLong) followed by amplification using the primers, T7FwdAMP and T7RevAMP. Pre-assembled PCR products were used as the substrate for the *in vitro* transcription. *In vitro* transcription of sgRNA was done using HiScribe T7 High Yield RNA Synthesis Kit (New England Biolabs, Inc.). RNA from *in vitro* transcription was purified using 5× solid phase reversible immobilization (SPRI) beads. The synthesized RNA concentration was measured using the Qubit RNA assay kit (Life Technologies, Inc).

AAVS1 sgRNA-1 oligo: ggatcctaatacactcactatagCCGGCCCTGGGAATATAAGGgttttagactagaa

POT1 sgRNA1 oligo: ggatcctaatacactcactatagGAGATCTTGCCACATGAACAgtttagactagaa

POT1 sgRNA2 oligo: ggatcctaatacactcactatagGTGATTTAAGTCACATCCATgttttagactagaa

(sgRNA sequences are in capital letters)

T7RevLong: AAAAAAGCACCGACTCGGTGCCACTTTTTCAAGTTGATAACGGACTAGCCTTATTTAACTTGCTATTTCTAGCTCTAAAAAC

T7FwdAMP: GGATCCTAATACGACTCACTATAG

T7RevAMP: AAAAAAGCACCGACTCGG

For targeting in hESCs, the following oligos were used for sgRNA production:

POT1 Y223C for insertion of PGK-Puro-pA cassette: GAGATCTTGCCACATGAACA

POT1 Y223C targeting removal of drug resistance via *de novo* proto-spacer adjacent motive (PAM) sites: GAGATCTTGCCACATGACCA and GTCTGCGATAATCATGTCCA

POT1 Q623H: GATTACATCTTCTGCAACTG

### Electroporation for genome editing

Genome editing by electroporation using Lonza 4D nucleofector was performed as described by the manufacturer's protocol (Lonza, Inc.). To validate sgRNA in K562, approximately 200,000 cells were pelleted and resuspended in 20  $\mu$ l of Lonza SF buffer containing supplement solution. The RNP complex was prepared by slowly adding 60 pmol of synthesized sgRNA to 100 pmol of purified CAS9 protein in CAS9 buffer. The RNP complex was incubated at room temperature for 20 min and was added to the cell suspension. To edit hCD34<sup>+</sup> cells, 1 million cells were resuspended in 100  $\mu$ l of Lonza P3 buffer containing supplement solution. RNP complex was prepared with 300 pmol of synthesized sgRNA and 500 pmol of purified CAS9 buffer as described above. The electroporation of K562 and hCD34<sup>+</sup> was done using a K562-specific program or program ER100, respectively.

For "scarless" genome editing in hESCs, cells were first co-electroporated with a sgRNA-expressing plasmid (px330) targeting POT1 and a donor plasmid. The donor plasmid contained a PGK-Puro-pA cassette flanked by *de novo* NcoI sites and the Y223C mutation in one of the homology arms. After selection with puromycin for 10 days, single cell-derived colonies were isolated, replicates were plated, and genomic DNA was isolated for confirmation of genotypes. The "scarless loopout" of correctly Puro-targeted clones was performed in a subsequent second step by co-electroporating a GFP expression plasmid (N2-GFP) with two px330 sgRNA-expressing plasmids targeting the two unique PAM sequences created by the NcoI sites. Cells were single cell-sorted for GFP expression and colonies were isolated and genotyped to confirm the removal of puromycin cassette while leaving behind the mutation (Y223C). Targeting was confirmed first by PCR and then by Sanger sequencing.

### Genotyping and sequencing

Y223C/–: Extracted genomic DNA from individual clones was amplified by PCR with the following primers sets and then digested with EcoRV to detect cell lines that were correctly targeted with both the Y223C mutation and the *de novo* EcoRV site. Amplified fragments that were not incubated with enzyme were then submitted for sequencing with one of the two primers in each set:

F1: cggtttgagaagaaaagc

R1: ccttcagagatctgcccaca

F2: tgccaatattcagagcataa

R2: ccagtttaccagcttagcattt

Q623H: Extracted genomic DNA was amplified by PCR with primers **ttaaatlttgaaggacgttt** and **actttattaggttgaggtg** and then digested with BglII for genotyping. Undigested PCR product was submitted for sequencing using one of the two primers. To ensure the accuracy of our genotyping and rule out the expansion of a subpopulation, we genotyped our cells at the end of the telomere length experiments. In addition, we subcloned genotyping PCR amplicons into PCR2.1. Sequencing of these plasmids supported all our genotyping results.

WT/Y223C: Initial insertion of the puromycin cassette was detected by PCR, where genomic DNA was extracted from individual clones and amplified by PCR using primers

**tgccaatattcagaggcataag** and **gcctttttcattctaaagcag**, and amplified products were submitted for sequencing using one of the two primers. A correctly targeted clone was identified and subject to two CAS9 guide RNAs targeted the *de novo* NcoI sites flanking the puromycin cassette, removing this by “scarless loopout”. After this round of targeting, extracted genomic DNA was amplified by PCR using primers **gtccgtctgcagggtacta** and **gccatatctaaactgtgcacct**, where a loss of a band indicated the removal of the puromycin cassette and successful targeting.

### **In vitro differentiation**

hCD34<sup>+</sup> cells were differentiated into erythroid lineage using established differentiation protocols (Giarratana *et al*, 2005; DeWitt *et al*, 2016). Briefly, hCD34<sup>+</sup> cells were cultured in IMDM supplemented with 5% human AB serum, heparin (2 IU/ml), human insulin (10 µg/ml), human holo-transferrin (330 µg/ml), recombinant human erythropoietin (3 unit/ml), hydrocortisone (1 µM), recombinant human stem cell factor (100 ng/ml), and human interleukin-3 (5 ng/ml) for 7 days. For colony-forming clonal expansion, CD34<sup>+</sup> cells were seeded in methylcellulose-based medium (MethoCult Express 04437, StemCell Technologies). In order to characterize colonies arising from single cells, cells were plated using limited dilution on 96-well plates. 2–3 weeks after seeding, single colonies were collected and genotyped by Sanger sequencing or NGS.

### **Xenotransplantation**

NBSGW mice from Jackson laboratory were used for the *in vivo* studies under the protocol approved by the office of laboratory animal care (OLAC) in UC Berkeley. Electroporated hCD34<sup>+</sup> cells were injected to 6- to 12-week-old gender-matched mice via tail vein. To monitor human chimerism, mice blood was collected from submandibular vein into EDTA-coated collection tubes after transplantation. Red blood cells were lysed using EL buffer (QIAGEN) and washed twice with phosphate-buffered saline (PBS). Recipient mice were euthanized at weeks 16–20 post-transplantation. Bone marrow cells were collected from femur and tibia. In these isolations, we did not observe any overt indications for hematopoietic neoplasia. For *ex vivo* culture, hCD34<sup>+</sup> cells from bone marrow were sorted using FACS Aria Fusion (BD Biosciences) and cultured using limited dilution culture method in methylcellulose-based medium on 96-well plate for 3 weeks.

### **Genotyping and NGS analysis**

Genomic DNA of human cells from *in vivo* and *in vitro* assays was isolated using Cell and Tissue DNA Micro Kit (Norgen Biotek). ~250 bp region around the CAS9 target site was amplified with primers (POT1-NGSF, POT1-NGSR, AAVS1-NGSF, and AAVS1-NGSR) containing stub sequence for Illumina TruSeq adaptor ligation. After subsequent adaptor ligation reaction, the library was run on a Illumina MiSeq sequencer using paired-end 150-cycle read. MiSeq reads were de-multiplexed using a custom analysis workflow script and analyzed using CRISPResso, a free online tool (Pinello *et al*, 2016).

POT1 NGSF: GCTCTCCGATCTAAACTACTCTACTCTTATGGCA  
POT1 NGSR: GCTCTCCGATCTaaattcatagcaaaaatcact

AAVS1 NGSF: GCTCTCCGATCTcccctatgtccacttcagga  
AAVS1 NGSR: GCTCTCCGATCTggaatctgcttaacaggaggt

### **Flow cytometry and sorting strategy**

100–200 µl of homogenized spleen or peripheral blood was treated with 2 ml of EL buffer (QIAGEN) for 1 min to lyse red blood cells. The reaction was quenched by adding 5–6 volume of chilled PBS. After centrifugation and removing supernatant, cells were stained with specific surface marker antibodies. The following antibodies (BD Biosciences) were used: V450 mouse anti-human CD19 (BD 560353), PE rat-anti-mouse CD45 (BD 553081), PE-Cy7 mouse anti-human CD34 (BD 348791), and FITC mouse anti-human CD45 (BD 555482). The cells were sorted using FACS Aria Fusion instrument. FACS data were analyzed using FlowJo software.

### **Single telomere length analysis (STELA)**

STELA was performed as previously described (Baird *et al*, 2003). Briefly, at least 4 ng of genomic DNA was digested with EcoRI for 2 h. After ligation reaction with 0.9 µM telorette 3 linker and 400 unit of T4 DNA ligase overnight, the DNA was diluted to 250 pg/ul for STELA PCR. STELA PCR (94°C for 2 min, 25 cycles of 94°C for 15 s, 65°C for 30 s, 68°C for 10 min, and final extension 68°C for 20 min) was carried out with 0.5 µM of teltail, XpYpE2 primer, 1× Taq buffer with (NH<sub>4</sub>)<sub>2</sub>SO<sub>4</sub>, 250 pg of ligated genomic DNA, 0.3 mM of dNTP, 1.5 mM of MgCl<sub>2</sub>, and DNA polymerase mix (Taq:Pwo, = 10:1). The PCR products were subjected to electrophoresis on a 0.5% agarose gel and transferred to Amersham Hybond-XL membrane (GE Healthcare). The PCR products on the membrane were hybridized with radio-labeled XpYp subtelomeric probe amplified using primers XpYpE2 and XpYpB2 and visualized with an Amersham Typhoon using a phosphor imager screen.

Telorette 3: TGCTCCGTGCATCTGGCATCCCTAACC  
Teltail: TGCTCCGTGCATCTGGCATC  
XpYpE2: GTTGTCTCAGGGTCTAGTG  
XpYpB2: TCTGAAAGTGACCTATCAG

### **Telomere restriction fragment analysis (TRF analysis)**

TRF analysis was performed as previously described (Boyle *et al*, 2020). Briefly, genomic DNA was digested with MboI, AluI, and RNaseA overnight at 37°C and separated on a 0.75% agarose gel, dried under vacuum for 2 h at 50°C, denatured in 0.5 M NaOH and 1.5 M NaCl for 30 min, shaking at 25°C, and neutralized with 1 M Tris pH 6.0 and 2.5 M NaCl, shaking at 25°C, 2× for 15 min. Then, the gel was pre-hybridized in Church’s buffer (1% BSA, 1 mM EDTA, 0.5 M NaPO<sub>4</sub> pH 7.2, 7% SDS) for 1 h at 55°C before adding a <sup>32</sup>P-end-labeled (C<sub>3</sub>TG<sub>2</sub>)<sub>3</sub> telomeric probe. The gel was washed 3 × 30 min in 4× SSC at 50°C and 1 × 30 min in 4× SSC + 0.1% SDS at 25°C before exposing on a phosphor imager screen.

### **T7 endonuclease I assay**

Genomic locus targeted by sgRNA was amplified by PCR. The PCR products were prepared in 20 µl volume containing NEB buffer 2

(New English Biolabs, Inc). Prior to T7 endonuclease treatment, the purified PCR product was denatured at 95°C for 5 min and annealed back by slowly cooling down to room temperature. After treating with 5 units of T7 endonuclease I for 30 min at 37°C, the final product was separated by electrophoresis and visualized.

### IF/TIF analysis

Analysis was carried out as previously described in Boyle *et al* (2020). For analysis by IF, cells were washed with PBS, fixed with 2% paraformaldehyde in PBS, permeabilized with 0.1% Triton X-100, and blocked with 1 mg/ml BSA, 3% v/v horse serum, and 1 mM EDTA in PBS. After blocking, cells were incubated with antibodies against TRF1 raised in rabbit against amino acid residues 17-41 (856-R1) and  $\gamma$ -H2AX (Millipore) in blocking solution followed by secondary antibodies. Scoring of TIF-positive cells was performed single blind. More than 50 cells were evaluated for each condition. *p*-values were determined using Prism 9's Mann-Whitney test. As a positive control and to demonstrate that these cells are competent to form TIFs, we infected them with a lentivirus expressing TPP1 $\Delta$ PBD or an empty control virus and stained them for TIFs 72 h post-infection. Cells not infected with the virus remained TIF negative.

### Metaphase Spreads/FISH

Analysis was carried out as previously described in Boyle *et al*, (2020). Cells were treated with colcemid at 100 ng/ml for 2 h. We collected the cells using trypsin and incubated at 37°C in prewarmed 75 mM KCl. The cells were spun down, and the KCl was removed. Cells were slowly resuspended in a fixative of 3:1 methanol:acetic acid. Cells were stored overnight at 4°C. The next day, cells were spread, dropwise, onto microscope slides and washed twice with 1 ml 3:1 methanol:acetic acid solution. Slides were then placed onto an 80°C humidified heat block for 5 min. Samples were fixed in 3.7% formaldehyde diluted in PBS and then treated with pepsin (1 mg/ml) prepared in 10 mM glycine pH 2 and warmed up to 37 degrees. After one more wash in 4% PFA, slides were washed with PBS and then dehydrated in an ethanol series. Each slide received 100  $\mu$ l of hybridization mixture, was denatured at 80 degrees for 5 min, and then hybridized overnight with Cy3 Tel-C probes (PNA Bio) at 4 degrees in a hybridization chamber. The next day, the slides were washed with 70% formamide, 10 mM Tris-HCl pH 7.2, and 0.1% BSA solution, then with 0.1 M Tris-HCl pH 2, 0.15 M NaCl, and 0.08% Tween, and with DAPI (diluted 1:1,000 from 5 mg/ml stock) added to the second wash. Coverslips were mounted with ProLong® Gold Antifade Mountant (Thermo Fisher Scientific). All microscopy (IF and metaphase spreads) was imaged on a Nikon Eclipse TE2000-E epifluorescent microscope equipped with an Andor Zyla sCMOS camera.

## Data availability

This study includes no data deposited in external repositories.

**Expanded View** for this article is available online.

## Acknowledgements

D.H. is a Chan Zuckerberg Biohub Investigator and supported by a Research Scholar Grants from the American Cancer Society (133396-RSG-19-029-01-DMC). D.H. is a Pew-Stewart Scholar for Cancer Research supported by the Pew Charitable Trusts and the Alexander and Margaret Stewart Trust. D.H. is supported by the Siebel Stem Cell Institute, the N.I.H. (R01-CA196884), and the D.O.D. (W81XWH-19-1-0586). MLM is supported by the Intramural Research Program of the Division of Cancer Epidemiology and Genetics of the National Cancer Institute, Bethesda, MD.

## Author contributions

W-TK, KH, JJ, RF, SC, MM, and DH planned experiments. DH wrote the paper with the help of KH, SC, and MLM. All HSC experiments were performed by W-TK. HESC experiments were performed and analyzed by KH, JJ, and BF with the help of SC, SBS, and CD.

## Conflict of interest

The authors declare that they have no conflict of interest.

## References

- Allsopp RC, Harley CB (1995) Evidence for a critical telomere length in senescent human fibroblasts. *Exp Cell Res* 219: 130–136
- Allsopp RC, Vaziri H, Patterson C, Goldstein S, Younglai EV, Futcher AB, Greider CW, Harley CB (1992) Telomere length predicts replicative capacity of human fibroblasts. *Proc Natl Acad Sci USA* 89: 10114–10118
- Artandi SE, Chang S, Lee SL, Alson S, Gottlieb GJ, Chin L, DePinho RA (2000) Telomere dysfunction promotes non-reciprocal translocations and epithelial cancers in mice. *Nature* 406: 641–645
- Artandi SE, DePinho RA (2000) A critical role for telomeres in suppressing and facilitating carcinogenesis. *Curr Opin Genet Dev* 10: 39–46
- Baird DM, Rowson J, Wynford-Thomas D, Kipling D (2003) Extensive allelic variation and ultrashort telomeres in senescent human cells. *Nat Genet* 33: 203–207
- Baumann P, Cech TR (2001) Pot1, the putative telomere end-binding protein in fission yeast and humans. *Science* 292: 1171–1175
- Baumann P, Podell E, Cech TR (2002) Human Pot1 (protection of telomeres) protein: cytolocalization, gene structure, and alternative splicing. *Mol Cell Biol* 22: 8079–8087
- Blasco MA, Lee HW, Hande MP, Samper E, Lansdorp PM, DePinho RA, Greider CW (1997) Telomere shortening and tumor formation by mouse cells lacking telomerase RNA. *Cell* 91: 25–34
- Bodnar AG, Ouellette M, Frolkis M, Holt SE, Chiu CP, Morin GB, Harley CB, Shay JW, Lichtsteiner S, Wright WE (1998) Extension of life-span by introduction of telomerase into normal human cells. *Science* 279: 349–352
- Boyle JM, Hennick KM, Regalado SG, Vogan JM, Zhang X, Collins K, Hockemeyer D (2020) Telomere length set point regulation in human pluripotent stem cells critically depends on the shelterin protein TPP1. *Mol Biol Cell* 31: 2583–2596
- Chakravarti D, LaBella KA, DePinho RA (2021) Telomeres: history, health, and hallmarks of aging. *Cell* 184: 306–322
- Chen C, Gu P, Wu J, Chen X, Niu S, Sun H, Wu L, Li Na, Peng J, Shi S *et al* (2017) Structural insights into POT1-TPP1 interaction and POT1 C-terminal mutations in human cancer. *Nat Commun* 8: 14929
- Chiba K, Lorbeer FK, Shain AH, McSwiggen DT, Schruf E, Oh A, Ryu J, Darzacq X, Bastian BC, Hockemeyer D (2017) Mutations in the promoter of the



- telomerase gene TERT contribute to tumorigenesis by a two-step mechanism. *Science* 357: 1416–1420
- Counter CM, Avilion AA, Lefeuve CE, Stewart NG, Greider CW, Harley CB, Bacchetti S (1992) Telomere shortening associated with chromosome instability is arrested in immortal cells which express telomerase activity. *EMBO J* 11: 1921–1929
- d'Adda di Fagnana F, Reaper PM, Clay-Farrace L, Fiegler H, Carr P, Von Zglinicki T, Saretzki G, Carter NP, Jackson SP (2003) A DNA damage checkpoint response in telomere-initiated senescence. *Nature* 426: 194–198
- Damle RN, Batliwalla FM, Ghiotto F, Valetto A, Albesiano E, Sison C, Allen SL, Koltitz J, Vinciguerra VP, Kudalkar P et al (2004) Telomere length and telomerase activity delineate distinctive replicative features of the B-CLL subgroups defined by immunoglobulin V gene mutations. *Blood* 103: 375–382
- De Ravin SS, Reik A, Liu P-Q, Li L, Wu X, Su L, Raley C, Theobald N, Choi U, Song AH et al (2016) Targeted gene addition in human CD34(+) hematopoietic cells for correction of X-linked chronic granulomatous disease. *Nat Biotechnol* 34: 424–429
- DeKaveler RC, Choi VM, Moehle EA, Paschon DE, Hockemeyer D, Meijising SH, Sancak Y, Cui X, Steine EJ, Miller JC et al (2010) Functional genomics, proteomics, and regulatory DNA analysis in isogenic settings using zinc finger nuclease-driven transgenesis into a safe harbor locus in the human genome. *Genome Res* 20: 1133–1142
- Denchi EL, de Lange T (2007) Protection of telomeres through independent control of ATM and ATR by TRF2 and POT1. *Nature* 448: 1068–1071
- DeWitt MA, Magis W, Bray NL, Wang T, Berman JR, Urbinati F, Heo S-J, Mitros T, Munoz DP, Boffelli D et al (2016) Selection-free genome editing of the sickle mutation in human adult hematopoietic stem/progenitor cells. *Sci Transl Med* 8: 360ra134
- Escudero L, Cleal K, Ashelford K, Fegan C, Pepper C, Liddiard K, Baird DM (2019) Telomere fusions associate with coding sequence and copy number alterations in CLL. *Leukemia* 33: 2093–2097
- Giarratana MC, Kobari L, Lapillonne H, Chalmers D, Kiger L, Cynober T, Marden MC, Wajcman H, Douay L (2005) Ex vivo generation of fully mature human red blood cells from hematopoietic stem cells. *Nat Biotechnol* 23: 69–74
- Gong Y, Stock AJ, Liu Y (2020) The enigma of excessively long telomeres in cancer: lessons learned from rare human POT1 variants. *Curr Opin Genet Dev* 60: 48–55
- Greenberg RA, Chin L, Femino A, Lee KH, Gottlieb GJ, Singer RH, Greider CW, DePinho RA (1999) Short dysfunctional telomeres impair tumorigenesis in the INK4a(delta2/3) cancer-prone mouse. *Cell* 97: 515–525
- Greider CW, Blackburn EH (1985) Identification of a specific telomere terminal transferase activity in Tetrahymena extracts. *Cell* 43: 405–413
- Gu P, Wang Y, Bisht KK, Wu L, Kukova L, Smith EM, Xiao Y, Bailey SM, Lei M, Nandakumar J et al (2017) Pot1 OB-fold mutations unleash telomere instability to initiate tumorigenesis. *Oncogene* 36: 1939–1951
- Harley CB, Futcher AB, Greider CW (1990) Telomeres shorten during ageing of human fibroblasts. *Nature* 345: 458–460
- He H, Li W, Comiskey DF, Liyanarachchi S, Nieminen TT, Wang Y, DeLap KE, Brock P, de la Chapelle A (2020) A truncating germline mutation of TINF2 in individuals with thyroid cancer or melanoma results in longer telomeres. *Thyroid* 30: 204–213
- Hockemeyer D, Daniels JP, Takai H, de Lange T (2006) Recent expansion of the telomeric complex in rodents: Two distinct POT1 proteins protect mouse telomeres. *Cell* 126: 63–77
- Hockemeyer D, Palm W, Else T, Daniels JP, Takai KK, Ye JZ, Keegan CE, de Lange T, Hammer GD (2007) Telomere protection by mammalian Pot1 requires interaction with Tpp1. *Nat Struct Mol Biol* 14: 754–761
- Hockemeyer D, Sfeir AJ, Shay JW, Wright WE, de Lange T (2005) POT1 protects telomeres from a transient DNA damage response and determines how human chromosomes end. *EMBO J* 24: 2667–2678
- Hockemeyer D, Soldner F, Beard C, Gao Q, Mitalipova M, DeKaveler RC, Katibah GE, Amora R, Boydston EA, Zeitler B et al (2009) Efficient targeting of expressed and silent genes in human ESCs and iPSCs using zinc-finger nucleases. *Nat Biotechnol* 27: 851–857
- Hockemeyer D, Wang H, Kiani S, Lai CS, Gao Q, Cassidy JP, Cost GJ, Zhang L, Santiago Y, Miller JC et al (2011) Genetic engineering of human pluripotent cells using TALE nucleases. *Nat Biotechnol* 29: 731–734
- Horn S, Figl A, Rachakonda PS, Fischer C, Sucker A, Gast A, Kadel S, Moll I, Nagore E, Hemminki K et al (2013) TERT promoter mutations in familial and sporadic melanoma. *Science* 339: 959–961
- Huang FW, Hodis E, Xu MJ, Kryukov GV, Chin L, Garraway LA (2013) Highly recurrent TERT promoter mutations in human melanoma. *Science* 339: 957–959
- Kim NW, Piatyszek MA, Prowse KR, Harley CB, West MD, Ho PL, Coviello GM, Wright WE, Weinrich SL, Shay JW (1994) Specific association of human telomerase activity with immortal cells and cancer. *Science* 266: 2011–2015
- Kipling D, Cooke HJ (1990) Hypervariable ultra-long telomeres in mice. *Nature* 347: 400–402
- Kolquist KA, Ellisen LW, Counter CM, Meyerson MM, Tan LK, Weinberg RA, Haber DA, Gerald WL (1998) Expression of TERT in early premalignant lesions and a subset of cells in normal tissues. *Nat Genet* 19: 182–186
- Lei M, Zaug AJ, Podell ER, Cech TR (2005) Switching human telomerase on and off with hPOT1 protein *in vitro*. *J Biol Chem* 280: 20449–20456
- Lengner CJ, Gimelbrant AA, Erwin JA, Cheng AW, Guenther MG, Welstead GG, Alagappan R, Frampton GM, Xu P, Muffat J et al (2010) Derivation of pre-X inactivation human embryonic stem cells under physiological oxygen concentrations. *Cell* 141: 872–883
- Lin TT, Letsolo BT, Jones RE, Rowson J, Pratt G, Hewamana S, Fegan C, Pepper C, Baird DM (2010) Telomere dysfunction and fusion during the progression of chronic lymphocytic leukemia: evidence for a telomere crisis. *Blood* 116: 1899–1907
- Lin TT, Norris K, Heppel NH, Pratt G, Allan JM, Allsup DJ, Bailey J, Cawkwell L, Hills R, Grimstead JW et al (2014) Telomere dysfunction accurately predicts clinical outcome in chronic lymphocytic leukaemia, even in patients with early stage disease. *Br J Haematol* 167: 214–223
- Loayza D, de Lange T (2003) POT1 as a terminal transducer of TRF1 telomere length control. *Nature* 423: 1013–1018
- Lombardo A, Genovese P, Beausejour CM, Colleoni S, Lee Y-L, Kim KA, Ando D, Urnov FD, Galli C, Gregory PD et al (2007) Gene editing in human stem cells using zinc finger nucleases and integrase-defective lentiviral vector delivery. *Nat Biotechnol* 25: 1298–1306
- Maciejowski J, de Lange T (2017) Telomeres in cancer: tumour suppression and genome instability. *Nat Rev Mol Cell Biol* 18: 175–186
- McIntosh BE, Brown ME, Duffin BM, Maufort JP, Vereide DT, Slukvin II, Thomson JA (2015) Nonirradiated NOD, B6.SCID Il2rgamma<sup>-/-</sup> Kit(W41/W41) (NBSGW) mice support multilineage engraftment of human hematopoietic cells. *Stem Cell Reports* 4: 171–180
- McMaster ML, Sun C, Landi MT, Savage SA, Rotunno M, Yang XR, Jones K, Vogt A, Hutchinson A, Zhu B et al (2018) Germline mutations in Protection of Telomeres 1 in two families with Hodgkin lymphoma. *Br J Haematol* 181: 372–377
- Nandakumar J, Bell CF, Weidenfeld I, Zaug AJ, Leinwand LA, Cech TR (2012) The TEL patch of telomere protein TPP1 mediates telomerase recruitment and processivity. *Nature* 492: 285–289

- Pinello L, Canver MC, Hoban MD, Orkin SH, Kohn DB, Bauer DE, Yuan GC (2016) Analyzing CRISPR genome-editing experiments with CRISPResso. *Nat Biotechnol* 34: 695–697
- Pinzaru A, Hom R, Beal A, Phillips A, Ni E, Cardozo T, Nair N, Choi J, Wuttke D, Sfeir A et al (2016) Telomere replication stress induced by POT1 inactivation accelerates tumorigenesis. *Cell Rep* 15: 2170–2184
- Pinzaru AM, Kareh M, Lamm N, Lazzarini-Denchi E, Cesare AJ, Sfeir A (2020) Replication stress conferred by POT1 dysfunction promotes telomere relocalization to the nuclear pore. *Genes Dev* 34: 1619–1636
- Ramsay AJ, Quesada V, Foronda M, Conde L, Martínez-Trillos A, Villamor N, Rodríguez D, Kwarciak A, Garabaya C, Gallardo M et al (2013) POT1 mutations cause telomere dysfunction in chronic lymphocytic leukemia. *Nat Genet* 45: 526–530
- Rice C, Shastrula PK, Kossenkov AV, Hills R, Baird DM, Showe LC, Doukov T, Janicki S, Skordalakes E (2017) Structural and functional analysis of the human POT1-TPP1 telomeric complex. *Nat Commun* 8: 14928
- Robles-Espinoza CD, Harland M, Ramsay AJ, Aoude LG, Quesada V, Ding Z, Pooley KA, Pritchard AL, Tiffen JC, Petljak M et al (2014) POT1 loss-of-function variants predispose to familial melanoma. *Nat Genet* 46: 478–481
- Rode L, Nordestgaard BG, Bojesen SE (2016) Long telomeres and cancer risk among 95 568 individuals from the general population. *Int J Epidemiol* 45: 1634–1643
- Roos G, Kröber A, Grabowski P, Kienle D, Bühler A, Döhner H, Rosenquist R, Stilgenbauer S (2008) Short telomeres are associated with genetic complexity, high-risk genomic aberrations, and short survival in chronic lymphocytic leukemia. *Blood* 111: 2246–2252
- Rossi D, Lobetti Bodoni C, Genuardi E, Monitillo L, Drandi D, Cerri M, Deambrogi C, Ricca I, Rocci A, Ferrero S et al (2009) Telomere length is an independent predictor of survival, treatment requirement and Richter's syndrome transformation in chronic lymphocytic leukemia. *Leukemia* 23: 1062–1072
- Rudolph P, Schubert C, Tamm S, Heidorn K, Hauschild A, Michalska I, Majewski S, Krupp G, Jablonska S, Parwaresch R (2000) Telomerase activity in melanocytic lesions: a potential marker of tumor biology. *Am J Pathol* 156: 1425–1432
- Schmutz IA-O, Mensenkamp AA-OX, Takai KK, Haadsma M, Spruijt L, de Voer RM, Choo SS, Lorbeer FA-O, van Grinsven EJ, Hockemeyer DA-O et al (2020) TIN2 is a haploinsufficient tumor suppressor that limits telomere length. *eLife* 9: e61235
- Sexton AN, Regalado SG, Lai CS, Cost GJ, O'Neil CM, Urnov FD, Gregory PD, Jaenisch R, Collins K, Hockemeyer D (2014) Genetic and molecular identification of three human TPP1 functions in telomerase action: recruitment, activation, and homeostasis set point regulation. *Genes Dev* 28: 1885–1899
- Shain AH, Yeh I, Kovalyshyn I, Sriharan A, Talevich E, Gagnon A, Dummer R, North J, Pincus L, Ruben B et al (2015) The genetic evolution of melanoma from precursor lesions. *N Engl J Med* 373: 1926–1936
- Shi J, Yang XR, Ballew B, Rotunno M, Calista D, Fagnoli MC, Ghiorzo P, Bressac-de Paillerets B, Nagore E, Avril MF et al (2014) Rare missense variants in POT1 predispose to familial cutaneous malignant melanoma. *Nat Genet* 46: 482–486
- Soldner F, Hockemeyer D, Beard C, Gao Q, Bell GW, Cook EG, Hargus G, Blak A, Cooper O, Mitalipova M et al (2009) Parkinson's disease patient-derived induced pluripotent stem cells free of viral reprogramming factors. *Cell* 136: 964–977
- Speedy HE, Di Bernardo MC, Sava GP, Dyer MJS, Holroyd A, Wang Y, Sunter NJ, Mansouri L, Juliusson G, Smedby KE et al (2014) A genome-wide association study identifies multiple susceptibility loci for chronic lymphocytic leukemia. *Nat Genet* 46: 56–60
- Takai H, Smogorzewska A, de Lange T (2003) DNA damage foci at dysfunctional telomeres. *Curr Biol* 13: 1549–1556
- Takai KK, Kibe T, Donigian JR, Frescas D, de Lange T (2011) Telomere protection by TPP1/POT1 requires tethering to TIN2. *Mol Cell* 44: 647–659
- Wang F, Podell ER, Zaugg AJ, Yang YT, Baciú P, Cech TR, Lei M (2007) The POT1-TPP1 telomere complex is a telomerase processivity factor. *Nature* 445: 506–510
- Wright WE, Piatyszek MA, Rainey WE, Byrd W, Shay JW (1996) Telomerase activity in human germline and embryonic tissues and cells. *Dev Genet* 18: 173–179
- Xin H, Liu D, Wan M, Safari A, Kim H, Sun W, O'Connor MS, Songyang Z (2007) TPP1 is a homologue of ciliate TEBP-beta and interacts with POT1 to recruit telomerase. *Nature* 445: 559–562
- Xin H, Liu D, Songyang Z (2008) The telosome/shelterin complex and its functions. *Genome Biol* 9: 232
- Ye JZ, Hockemeyer D, Krutchinsky AN, Loayza D, Hooper SM, Chait BT, de Lange T (2004) POT1-interacting protein PIP1: a telomere length regulator that recruits POT1 to the TIN2/TRF1 complex. *Genes Dev* 18: 1649–1654
- Zhong FL, Batista LF, Freund A, Pech MF, Venteicher AS, Artandi SE (2012) TPP1 OB-fold domain controls telomere maintenance by recruiting telomerase to chromosome ends. *Cell* 150: 481–494



**License:** This is an open access article under the terms of the Creative Commons Attribution-NonCommercial-NoDerivs 4.0 License, which permits use and distribution in any medium, provided the original work is properly cited, the use is non-commercial and no modifications or adaptations are made.